

C₆₀-based hot-electron magnetic tunnel transistor

M. Gobbi,^{1,a)} A. Bedoya-Pinto,¹ F. Golmar,^{1,2} R. Llopis,¹ F. Casanova,^{1,3} and L. E. Hueso^{1,3}

¹CIC nanoGUNE Consolider, Tolosa Hiribidea 76, 20018 Donostia - San Sebastian, Spain

²I.N.T.I.-CONICET, Av. Gral. Paz 5445, Ed. 42, B1650JKA, San Martín, Bs As, Argentina

³IKERBASQUE, Basque Foundation for Science, 48011 Bilbao, Spain

(Received 19 July 2012; accepted 20 August 2012; published online 4 September 2012)

A C₆₀-based magnetic tunnel transistor is presented. The device is based on the collection of spin-filtered hot-electrons at a metal/C₆₀ interface, and it allows an accurate measurement of the energy level alignment at such interface. A 89% change in the collected current under the application of a magnetic field demonstrates that these devices can be used as sensitive magnetic field sensors compatible with soft electronics. © 2012 American Institute of Physics.

[<http://dx.doi.org/10.1063/1.4751030>]

Carbon-based materials, characterized by long spin coherence times, are promising candidates for next generation spintronics. On one hand, graphene and carbon nanotubes have typically high carrier mobilities and long mean free paths which translate into extremely large spin diffusion lengths. Therefore, they are template materials for applications in which the spin signal needs to be conserved over long distances.^{1–4} On the other hand, the combination between ferromagnetic (FM) metals and molecules offers the possibility to design spintronic devices with additional functionalities.⁵ Indeed, diverse organic semiconductors have been used as spacers between ferromagnetic layers, constituting the building blocks of spin-valve structures with very high figures of merit.^{6–11} Such spin-valve devices can be used as highly sensitive sensors and can be integrated in soft electronics circuitry, finding applications in the emerging field of flexible spintronics.¹² In these spintronic devices, the interface between the ferromagnetic metal and the carbon-based material plays a fundamental role.^{13,14} In particular, it has been shown that the energy level alignment at the metal/molecule interface affects not only the electrical conduction but also the spin polarization of the current.⁷

In this letter, we report a hot-electron magnetic tunnel transistor (MTT) which employs C₆₀ as semiconducting channel, and we show two very different applications of such device. First, the device structure allows the direct measurement of the metal/molecule energy level alignment in a ballistic electron emission spectroscopy experiment. Second, the output electrical current is extremely sensitive to small magnetic fields, making it suitable for sensing applications.

MTTs are 3-terminal devices with the same scheme of a metal base transistor, in which a hot-electron current is injected into the device by an emitter, and a spin-valve base modulates the amount of current reaching the semiconducting collector (Fig. 1).^{15,16} The device is based on the spin filtering effect of a thin FM layer on hot electron currents. The energy attenuation length of hot-electrons in a FM layer is spin dependent, so that minority electrons lose their energy much faster than majority electrons.¹⁵ The spin polarization of the hot-electron current can thus exceed 90% for FM

layers thicker than 3 nm.¹⁷ The Schottky barrier at the spin-valve/semiconductor interface is used to collect only those electrons that have retained their energy upon travelling through the base, i.e., the spin filtered electrons. When the spin-valve base is in parallel (P) state, a fraction of the majority electrons can travel through both layers without losing their energy, therefore getting collected as electrical current at the semiconducting terminal (Fig. 1(a)). When the spin-valve base is in anti-parallel (AP) state, electrons are filtered in either one or the other FM layer, leaving ideally a negligible current in the collector (Fig. 1(b)).¹⁵ Under these conditions, the current change in the collector due to the magnetic state of the spin valve is called magnetocurrent (MC) and is defined as

$$MC(\%) = 100 \times (I_p - I_{ap})/I_{ap}. \quad (1)$$

So far, only MTTs based on conventional bulk inorganic semiconductors such as Si or GaAs have been experimentally demonstrated.^{16–22} We produced and characterized MTTs employing C₆₀ as a semiconducting collector, taking advantage of the properties which make it ideal both for organic spintronic devices^{10,11,23} and for metal-base transistors.²⁴ In this study, we demonstrate that the C₆₀-based MTT perform as state-of-the-art inorganic MTT, with a room temperature MC reaching 89% at zero base-collector bias. Moreover, we show that this MC value can be enhanced by the

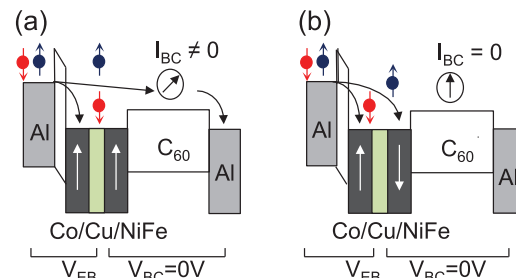


FIG. 1. The energy diagram of the device when the spin valve is in the parallel state (a) and in the antiparallel state (b). The emitter-base voltage V_{EB} determines the alignment of the Fermi Energy at the tunnel junction terminals, while at the metal/C₆₀ interface an energy barrier naturally forms. Under these conditions, and assuming a perfect spin filtering effect, the current enters the C₆₀ collector only when the spin valve is in the parallel state.

^{a)} Author to whom correspondence should be addressed. Electronic mail: m.gobbi@nanogune.eu.

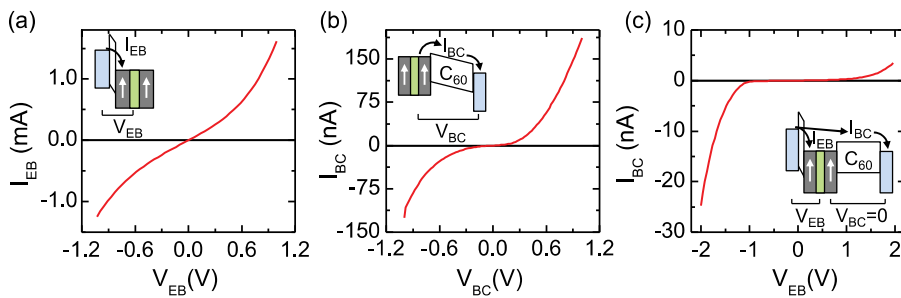


FIG. 2. I-V traces measured across the tunnel junction (a) and the C_{60} layer (b). (c) Hot-electron current I_{BC} measured at the collector terminal when the emitter-base voltage V_{EB} is swept and the base-collector voltage V_{BC} is kept at 0 V. Insets: energy diagrams to illustrate how the voltages are applied at the different terminals.

application of a proper voltage at the collector, reaching in principle an infinite value due to a negligible current in the off-state.

The devices were grown in an ultra-high vacuum dual chamber evaporator, with one chamber dedicated to the metal e-beam evaporation and the other one to the C_{60} thermal evaporation. In every chip, six devices were patterned by deposition through shadow masks on $10 \times 10 \text{ mm}^2$ SiO_2 (150 nm)/Si substrates. The emitter is composed by a 10-nm-thick Al layer, which is *in situ* plasma-oxidized to form an insulating AlO_x barrier at the interface with the metal base. The voltage V_{EB} applied at the tunnel junction (TJ) terminals defines the energy of the injected electrons (Fig. 1). This energy has to be set well above the Fermi energy of the base to generate a hot electron current. The base is a metallic spin valve, composed by a $\text{Co}(4 \text{ nm})/\text{Cu}(4 \text{ nm})/\text{Ni}_{80}\text{Fe}_{20}(4 \text{ nm})$ trilayer grown on top of the Al/AlO_x emitter (Fig. 1). The electrical resistance of the trilayer changes by a few percent (in our devices typically $<1\%$) depending on the relative alignment of the magnetization of the two FM layers (either parallel or antiparallel).^{25,26} The collector is a 200-nm-thick C_{60} layer with an Al top electrode for the actual electric contact placed above.

The current-voltage (I-V) characteristics of our devices are shown in Fig. 2. Fig. 2(a) shows the emitter-base current I_{EB} flowing through the TJ when the voltage V_{EB} is swept between the emitter and the spin-valve base. This non-linear I-V trace is typical of TJs. Fig. 2(b) shows the current I_{BC} flowing across the C_{60} layer when the voltage V_{BC} is applied directly between the base and the C_{60} top terminal. The 200-nm-thick C_{60} layer is highly resistive ($R > 20 \text{ M}\Omega$ at low bias voltage), and the I-V trace is again highly non-linear due to the energy barriers at the metal/organic interfaces. Finally, Fig. 2(c) shows the base-collector current I_{BC} when the voltage V_{EB} is swept at the emitter-base terminals (with zero set voltage across the C_{60} , $V_{BC} = 0$). In this case, I_{BC} is due to those hot electrons that have retained enough energy to overcome the barrier at the metal/ C_{60} interface. At low V_{EB} , I_{BC} is extremely small whereas it rises abruptly when the voltage V_{EB} is higher than the metal/semiconducting barrier. We highlight two important aspects: (1) the I-V trace of Fig. 2(c) is very different from both I-V traces measured either across the TJ and the C_{60} due to its different physical origin, namely the injection of hot electrons into the C_{60} . (2) The I-V trace is highly asymmetric and in particular we measure higher current when the emitter is negatively biased, i.e., it is injecting electrons and not holes. This is in good agreement with the well-accepted n-type nature of C_{60} ,

meaning that the majority carriers are electrons.²⁷ Furthermore, the attenuation length of hot holes in FM layers is from 2 to 5 times shorter than the electron attenuation length.²¹ This MTT device configuration allows a direct measurement of the energy level alignment at the C_{60} /base.²⁸ From the threshold voltage after which I_{BC} begins to rise (electrons with enough energy to enter the collector), we estimate the NiFe/C_{60} energy barrier to be around 1.0 eV.

We move now to the magnetic properties of the MTTs. First, we analyze the case in which a bias voltage is applied at the emitter-base terminals, with the collector kept at the same potential of the base. In this situation, the current measured at the collector displays the typical magnetoresistive behavior shown in Fig. 3(a). I_{BC} is at its maximum when the external magnetic field is strong enough to keep the FM layers in the base parallelly aligned. A minimum is reached

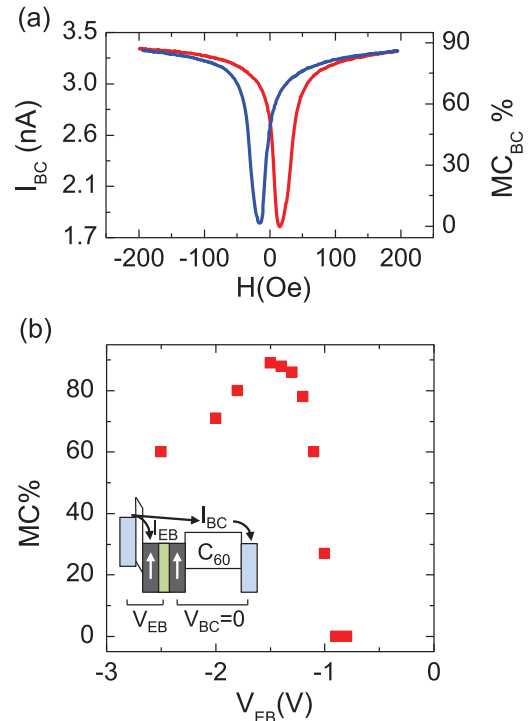


FIG. 3. (a) Base-collector current I_{BC} as a function of the applied magnetic field (measured at $V_{EB} = -1.4 \text{ V}$, $V_{BC} = 0 \text{ V}$). Red and blue traces correspond to negative to positive and positive to negative field sweep, respectively. On the right axis, the corresponding magnetocurrent. (b) Magnetocurrent as a function of the emitter-base voltage V_{EB} . Inset: Energy diagram showing how the voltages are applied for the measurement in (a) and (b).

when the alignment is antiparallel, giving rise to MC values up to 89% (Fig. 3(a)) at room temperature. As pointed out above, a naive analysis would expect the current in the AP state to be exactly zero (Fig. 1(b)), but this ideal case can hardly be realized in actual devices due to the leakage current I_{ap} which flows also in the AP state. For this reason, a MC value of 89% at room temperature is especially remarkable, as in many cases the leakage current is too high to even permit any sizable magnetic effect at room temperature.^{16,17,19–22} We highlight here that the injection of hot electrons through ferromagnetic layers is one of the most efficient methods to inject highly spin-polarized current into semiconductors.^{29,30} Under the assumption of a perfect spin filtering¹⁷ and no leakage current, the hot-electron current entering the semiconductor is 100% spin-polarized (see Fig. 1(a)). In our devices, considering the relatively low value of I_{ap} , we expect a high spin polarization of I_{BC} entering the C_{60} layer. However, in order to verify whether the spin polarization is maintained across the C_{60} layer, a different device geometry would be necessary.³⁰

The dependence of MC with the emitter-base bias voltage is shown in Fig. 3(b). In agreement with the I-V measurements (Fig. 2(c)), no hot-electron MC is recorded in the C_{60} collector for $V_{EB} > 0$. At negative voltages, the MC rises for $V_{EB} < -1$ V, being $V_{EB} = -1$ V the minimum bias needed to inject hot-electrons into the C_{60} . The MC bias dependence is non-monotonic and the maximum value of 89% is reached at $V_{EB} = -1.5$ V, while for more negative voltages the MC decreases. This behavior has been already observed in fully inorganic MTTs and has been explained using a model based on spin-dependent inelastic scattering in the FM layers of the base.¹⁹

Finally, we demonstrate that MC can be modulated by the application of a proper voltage between the base and the collector. The highest reported values of MC are measured at low temperatures when the leakage current flowing into the collector in the AP state is minimized.^{15–22} We show that a similar outcome can be obtained at room temperature by applying a base-collector voltage V_{BC} . Fig. 4(a) shows the MC change by varying V_{BC} while keeping V_{EB} constant. In the device shown in Fig. 4(a) we measured 50% MC with $V_{BC} = 0$. By setting $V_{BC} \neq 0$, an additional current contribution flows between the base and the collector. In the case of $V_{BC} < 0$ (i.e., accelerating the electrons in the C_{60} layer), the current reaching the collector increases because some electrons enter the C_{60} directly from the base. However, since these electrons do not have a hot origin, they do not actually improve the MC and they just add to the leakage current, effectively lowering the MC ratio (Fig. 4(b), negative voltages). In the case $V_{BC} > 0$, the current in the AP state (I_{ap}) shifts towards zero (Fig. 4(b)). As a consequence, the MC increases to values higher than 50% (Fig. 4(a), positive voltage). In that way, the MC curve can be arbitrarily displaced choosing the right V_{BC} value. In Fig. 4(b), we show how the MC curves evolve for three different selected V_{BC} ; the red curve corresponding to $V_{BC} = 0.135$ V has very low current in the AP state, giving rise to extremely high MC (8550%).

In conclusion, the realization of a magnetic tunnel transistor employing C_{60} as semiconducting layer has been demonstrated, with performances comparable to conventional

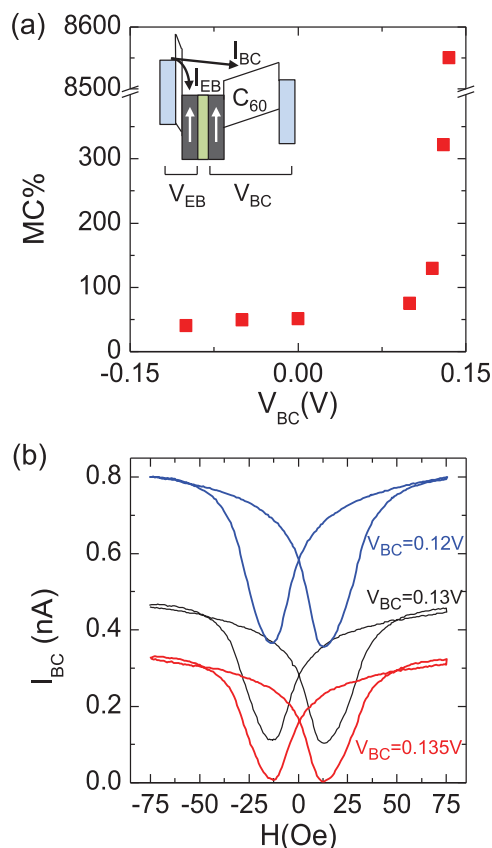


FIG. 4. (a) Dependence of the magnetocurrent with the base-collector voltage V_{BC} . Inset: Energy diagram showing how the voltages are applied for the measurements in (a) and (b). (b) Magnetocurrent curves for different V_{BC} values.

inorganic MTTs. We have recorded a zero-collector-bias magnetocurrent of 89% at room temperature, which can be increased to any arbitrary value by applying a voltage at the collector terminal. The device geometry allowed us to determine the energy barrier at the NiFe/ C_{60} interface, which is found to be 1 eV. We expect our results to be reproduced by other molecular semiconductors, opening additional pathways for the development of organic spintronics.

This work is supported by the European Union 7th Framework Programme (NMP3-SL-2011-263104-HINTS and PIRG06-GA-2009-256470), by the European Research Council (Grant No. 257654-SPINTROS), by the Spanish Ministry of Science and Education under Project No. MAT2009-08494, and by the Basque Government through Project No. PI2011-1.

¹B. Dlubak, M. B. Martin, C. Deranlot, B. Served, S. Xavier, R. Mattana, M. Sprinkle, C. Berger, W. A. De Heer, F. Petroff, A. Anane1, P. Seneor, and A. Fert, *Nat. Phys.* **8**, 557 (2012).

²W. W. Han, K. M. McCreary, K. Pi, W. H. Wang, Y. Li, H. Wen, J. R. Chen, and R. K. Kawakami, *J. Magn. Magn. Mater* **324**, 369 (2012).

³T. Maassen, J. J. van den Berg, N. Ijbema, F. Fromm, T. Seyller, R. Yakimova, B. J. van Wees, *Nano Lett.* **12**, 1498 (2012).

⁴L. E. Hueso, J. M. Pruneda, V. Ferrari, G. Burnell, J. P. Valdes-Herrera, B. D. Simons, P. B. Littlewood, E. Artacho, A. Fert, and N. D. Mathur, *Nature (London)*, **445**, 410 (2007).

⁵V. A. Dediu, L. E. Hueso, I. Bergenti, and C. Taliani, *Nat. Mater.* **8**, 707 (2009).

- ⁶Z. H. Xiong, D. Wu, Z. V. Vardeny, and J. Shi, *Nature (London)* **427**, 821 (2004).
- ⁷C. Barraud, P. Seneor, R. Mattana, S. Fusil, K. Bouzouhouane, C. Deranlot, P. Graziosi, L. Hueso, I. Bergenti, V. Dediu, F. Petroff, and A. Fert, *Nat. Phys.* **6**, 615 (2010).
- ⁸T. S. Santos, J. S. Lee, P. Migdal, I. C. Lekshmi, B. Satpati, and J. S. Moodera, *Phys. Rev. Lett.* **98**, 016601 (2007).
- ⁹V. Dediu, L. E. Hueso, I. Bergenti, A. Riminucci, F. Borgatti, P. Graziosi, C. Newby, F. Casoli, M. P. De Jong, C. Taliani, and Y. Zhan, *Phys. Rev. B* **78**, 115203 (2008).
- ¹⁰M. Gobbi, F. Golmar, R. Llopis, F. Casanova, and L. E. Hueso, *Adv. Mater.* **23**, 1609 (2011).
- ¹¹T. L. A. Tran, T. Q. Le, J. G. M. Sanderink, W. G. van der Wiel, and M. P. de Jong, *Adv. Funct. Mater.* **22**, 1180 (2012).
- ¹²C. Barraud, C. Deranlot, P. Seneor, R. Mattana, B. Dlubak, S. Fusil, K. Bouzouhouane, D. Deneuve, F. Petroff, and A. Fert, *Appl. Phys. Lett.* **96**, 072502 (2010).
- ¹³G. Schmidt, D. Ferrand, L. W. Molenkamp, A. T. Filip, and B. J. van Wees, *Phys. Rev. B* **62**, R4790 (2000).
- ¹⁴A. Fert, J.-M. George, H. Jaffrès, and R. Mattana, *IEEE Trans. Electron Devices* **54**, 921 (2007).
- ¹⁵R. Jansen, *J. Phys. D* **36**, R289 (2003).
- ¹⁶D. J. Monsma, J. C. Lodder, Th. J. A. Popma, and B. Dieny, *Phys. Rev. Lett.* **74**, 5260 (1995).
- ¹⁷S. van Dijken, X. Jiang, and S. S. P. Parkin, *Appl. Phys. Lett.* **83**, 951 (2003).
- ¹⁸R. Jansen, P. S. A. Kumar, O. M. J. van't Erve, R. Vlutters, P. de Haan, and J. C. Lodder, *Phys. Rev. Lett.* **85**, 3277 (2000).
- ¹⁹S. van Dijken, X. Jiang, and S. S. P. Parkin, *Phys. Rev. Lett.* **90**, 197203 (2003).
- ²⁰S. van Dijken, X. Jiang, S. S. P. Parkin, *J. Appl. Phys.* **97**, 043712 (2005).
- ²¹B. G. Park, E. Haq, T. Banerjee, B. C. Min, J. C. Lodder, and R. Jansen, *J. Appl. Phys.* **99**, 08S703 (2006).
- ²²T. Nagahama, H. Saito, and S. Yuasa, *Appl. Phys. Lett.* **96**, 112509 (2010).
- ²³M. Gobbi, A. Pascual, F. Golmar, R. Llopis, F. Casanova, and L. E. Hueso, *Org. Electron.* **13**, 366 (2012).
- ²⁴M. S. Meruvia, I. A. Hummelgen, M. L. Sartorelli, A. A. Pasa, and W. Schwarzacher, *Appl. Phys. Lett.* **84**, 3978 (2004).
- ²⁵M. N. Baibich, J. M. Broto, A. Fert, F. N. Van Dau, F. Petroff, P. Eitenne, G. Creuzet, A. Friederich, and J. Chazelas, *Phys. Rev. Lett.* **61**, 2472 (1988).
- ²⁶G. Binasch, P. Grünberg, F. Saurenbach, and W. Zinn, *Phys. Rev. B* **39**, 4828 (1989).
- ²⁷C. D. Dimitrakopoulos and P. R. L. Malenfant, *Adv. Mater.* **14**, 99 (2002).
- ²⁸J. S. Jiang, J. E. Pearson, and S. D. Bader, *Phys. Rev. Lett.* **106**, 156807 (2011).
- ²⁹X. Jiang, R. Wang, S. van Dijken, R. Shelby, R. Macfarlane, G. S. Solomon, J. Harris, and S. S. P. Parkin, *Phys. Rev. Lett.* **90**, 256603-1 (2003).
- ³⁰I. Appelbaum, B. Huang, and D. J. Monsma, *Nature (London)* **447**, 295 (2007).